INNOVATIONS

RADIATION DOSE OPTIMIZATION TECHNOLOGIES IN MULTIDETECTOR COMPUTED TOMOGRAPHY: A REVIEW

J. C. Ramirez-Giraldo[1], A. N. Primak[1], K. Grant[1], B. Schmidt[2], M. K. Fuld[1]

[1]Siemens Medical Solutions USA Inc., Malvern PA, USA; [2]Siemens Healthcare, Forchheim, Germany

***Abstract*—Computed tomography (CT) is a well stablished imaging technique that is used worldwide for diagnosis and treatment planning. The purpose of this review is to describe the most notable technological advances in the last decade, with a special focus on their impact in CT dose optimization, that is, achieving the same diagnostic image quality at a reduced radiation dose. The review describes main components of a CT system such as x-ray tubes, detectors, shape filters and collimators; as well as the control of key variables such as the tube current and tube potential. In addition, technological advances in iterative reconstruction and specific applications such as cardiac CT, ultra-fast scanning with dual-source CT, and dual-energy CT, are also presented. While the some topics discussed in this review could be generalized to all modern CT scanners, many features are specific for CT systems manufactured by Siemens Healthcare and thus might not be available through other manufacturers**.

Keywords— **Computed Tomography, radiation dose reduction, image quality, radiation dose optimization.**

I. Introduction

Since its introduction in the seventies [1], computed tomography (CT) technology has improved tremendously and has become an essential imaging modality for treatment planning and for the diagnosis of different pathologies such as cancer, infectious diseases, trauma, stroke, cardiovascular diseases, among others. Some notable advances over the first three decades after its introduction include the development of spiral (or helical) CT [2], multi-detector CT [3] [4], and the dual-source CT [5]. These technological advances have led to the establishment of CT as an imaging modality that provides isotropic and sub-millimeter spatial resolution, fast acquisition speeds -with typical acquisition times below 10 seconds for whole volumes of data-, and with routine temporal resolution as low as 65 ms [6] [7] for applications such as cardiac imaging. While the technologies aimed to improve acquisition speed, temporal resolution and spatial resolution continue to steadily progress, radiation dose reduction has only recently become a primary driver of the development of new CT technologies. In the last decade, radiation dose from imaging procedures that use ionizing radiation have received increased attention and scrutiny. A report from the National Council on Radiation Protection and Measurements (NCRP) indicated that the average effective dose per capita to the US population had increased from 3.6 mSv in 1980 to about 6.2 mSv in 2006 [8]. The same report identified that radiation from medical procedures was the primary reason for such increase, and that a contribution of about 24% to the effective dose per capita was due to CT alone [8]. These findings reflect the consolidation of CT as an essential imaging modality for diagnosis and treatment in modern medical practice. This consolidation is also supported by the fact that over 70 million CT examinations are performed per year in the US alone [9]. However, the increased utilization of CT and the small potential risk of cancer associated with the use of ionizing radiation [10], require that every CT scan is both clinically justified and performed using the CT technique optimized with respect to radiation dose [11]. In this paper, we will focus on the latter.

While dose reduction is important, acquiring a poor non diagnostic scan for the sake of having ultra-low dose provides no benefit to the patient. Thus to provide good patient care and maximize the benefits to patients, it is crucial to perform exams that reduce radiation dose while maintaining diagnostic image quality. Hence, we will focus on the most recent CT technologies which aim for exam optimization rather than a mere radiation dose reduction. To facilitate the description of newer CT technologies it is convenient to review the CT imaging chain (**Fig. 1**). It starts with the essential components of a CT system that include the x-ray tube (s), shape (bowtie) filters, collimators and detectors (Section II). Next, the CT scanner has various control systems, most notably for the x-ray tube current and tube potential. The control of these parameters have a direct impact both on the radiation dose used during a CT examination and the image quality, particularly regarding image noise and contrast-to-noise ratio (Section III). After the acquisition and prior to image reconstruction, the CT projection data undergoes several preprocessing steps (i.e. beam hardening and scatter correction), usually transparent to the end users of clinical systems. Finally, the image reconstruction takes place using either the traditional filtered backprojection (FBP) or iterative reconstruction (IR) methods (Section IV). In most cases several of the aforementioned technologies can be simultaneously combined to optimize radiation dose and image quality or be adapted for specific applications such as cardiac imaging, ultra-fast acquisition, or dual-energy CT (Section V). Newly introduced features such as dose structured reports, dose notifications and alerts are also discussed (Section VI).

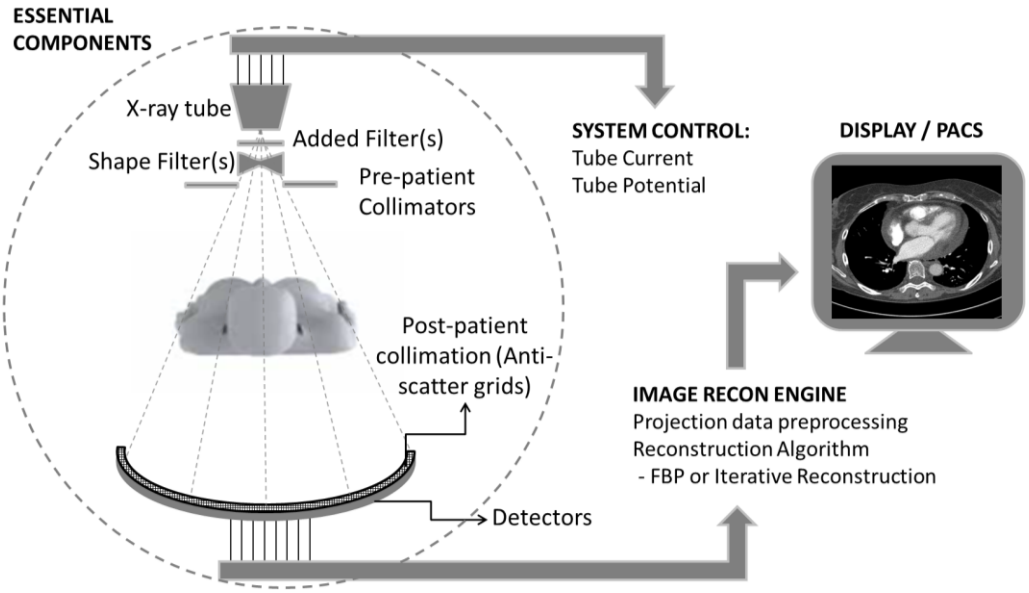

Fig. 1. Block diagram with some of the components of the CT system imaging chain.

II. CT SYSTEM HARDWARE

X-ray tube

An x-ray tube is one of the essential components of a CT system. The key characteristics that define the performance of an x-ray tube include tube power reserve, heat storage capacity, focal spot size, and the range of polychromatic spectra that it provides (i.e. the different kilovoltage values at which it can operate). Modern clinical CT systems typically operate at a peak power of between 50 to 80 kW, with higher end systems able to reach up to 120 kW per x-ray tube. Large power reserves of 80 kW or higher are particularly helpful for ultra-fast scanning modes and for scanning obese patients. In these applications, the x-ray tube must operate near its maximum current. Therefore, unless there's enough tube power, some decrease of the acquisition speed might be needed in order to be able to scan larger patients with sufficient image quality [12]. One solution to increase the overall tube power reserve is to use a dual-source (DS) CT system that can simultaneously and independently operate two perpendicularly arranged x-ray tubes. Such technology can double the power reserve up to 2 x 120 kW in the third generation DS system (SOMATOM Force®, Siemens Healthcare), when operating both tubes at the same kV [13].

A specific approach for the x-ray tube design is the rotating envelope tube (Straton®, Siemens Healthcare), which utilizes convective cooling rather than radiative cooling as in conventional rotating anode disks [14]. This design allows operations at a high-power with high heat dissipation rates of 5,400 kJ/min. Because of the fast cooling ability; rotating envelopes facilitate operation in rapid succession minimizing the need of cooling delays in between scans. Typical peak tube potential values available in modern CT scanners are from 80 to 140 kVp. Most recently, lower tube potential settings at 70 kVp (CARE Child, Siemens Healthcare, Forchheim, Germany) has been introduced and are particularly well suited for scanning children [15] or thinner structures in the body such as the neck [16].

One limitation of the Straton and other x-ray tubes is that it can only reach its maximum power at high tube potentials (e.g. 120 or 140 kV), while at low tube potentials (e.g. 80 and 100 kV) the maximum tube current (hence, power) is significantly smaller than at 120 kV. The newest x-ray tube (Vectron®, Siemens Healthcare) employed by the third generation DS system overcomes this limitation and can achieve a very high tube current up to 1300 mA, even at low tube potential values such as 70, 80 or 90 kV. This is a major advantage for low kV imaging that is often limited by insufficient power reserve [17].

X-ray beam shaping filters

Considering that the cross-section of patients is well approximated by an oval shape, special shape filters like the "bowtie filters" are nowadays common in CT systems for attenuating the beam at the periphery, while keeping the intensity in the central portion of the beam. Further adaptation of these bowtie filters can be considered for specific scanning modes such as pediatric imaging or cardiac imaging. For example, cardiac bowtie filters reduce the exposure outside of the area of the heart leading to lower dose in organs and structures outside of this area. Radiation dose savings due to bowtie filters have been reported to be in the range of 10 to 20% [18].

One of the effects of adding filters to the x-ray beam is that these filters can affect the x-ray spectra. For example, most x-ray tubes in a CT scanner include some added filtration such as aluminum to cut off the lower energy photons that typically do not contribute to image formation. Even shape filters can alter the x-ray spectra by a small percentage [19].

Primak et al. investigated the use of additional (flat) filters for the x-ray tube operating at high tube voltage for dual-source dual-energy CT applications [20]. The added filtration, of materials such as tin, increased the spectra separation between the tubes operating at low and high energies and was demonstrated to reduce image noise in material-specific dual-energy images, which in turn translated to dose reduction for dual-energy CT applications [21]. More recently, with the introduction of the third-generation DSCT (SOMATOM Force®, Siemens Healthcare), two special acquisition modes were included, in which a flat tin filter is added to both x-ray tubes operating at either 100 kVp or 150 kVp. For these modes, instead of achieving spectral separation between the low and high energies, the entire spectrum is shifted to higher energies. It was demonstrated that for non-contrast imaging tasks such as discriminating soft tissue and air that, this hardened spectra can be more dose efficient achieving a high contrast-to-noise ratio between soft tissue and air with less dose than traditional scan modes without the tin filter at typical tube voltages. Applications for the 100 kV with tin acquisition mode have already been demonstrated in phantoms and patients undergoing low-dose non-contrast chest CT with doses as low as 0.07 mSv, while still maintaining the ability to detect lung nodules [22].

Collimators

There are two basic types of collimators in CT: pre-patient and post-patient. Conventional approaches for both types of collimation are reviewed elsewhere [23] [24]. Some of the latest advances in pre-patient collimations are the dynamically adjustable z-axis x-ray beam collimators (e.g. Adaptive Dose Shield, Siemens Healthcare, Forchheim, Germany); which are used in spiral CT to reduce unnecessary dose due to overscanning [25] [26] [27]. In order to acquire sufficient data to reconstruct a particular image slice, it is necessary to acquire enough projection data before and after that slice (required for spiral interpolation). Therefore, a full irradiation of the detector through the slice is needed, although not all acquired data contributes to the final image formation. Dynamically adjustable z-axis collimation is achieved by using fast motion collimator blades that limits this over-scanning. At the beginning and end of each spiral CT scan, the pre-patient collimator asymmetrically opens and closes with the purpose of blocking the portions of the x-ray beam which do not provide the projection data useful for the image reconstruction. The use of this technology has been shown to lead to dose reductions in the range of 5 to 50% while maintaining image quality, with percent reductions strongly dependent on the pitch and scanning range [26]. The higher reductions were observed for scans using high-pitch values (and hence higher overscanning needed) and short scan ranges; as often would be the case in pediatric imaging and cardiac CT [28].

Detectors

Modern CT systems use solid-state detectors which are made of materials such as gadolinium oxide, cadmium tungstate or ultra-fast ceramics (UFC®, Siemens Healthcare) [29]. While the detector itself is the component which transduces absorbed x-rays into light, the whole detector module (or detector cell) is also comprised of a photodiode, which transduces light into an electric signal, and an analog-to-digital converter (ADC) that, as the name suggests, takes the analog electric signal produced by the photodiode and converts it into a digital signal. To improve radiation dose efficiency, advances in the detector material and system electronics are needed. One of those latest advances has been in the detector electronics by integrating the photodiode and ADC into one application-specific integrated circuit (ASIC). The benefit of this integration is that it obviates analog connections of conventional detector electronics, which are a major source of electronic noise. Quantum noise is typically they main contributor to CT image noise and is determined by the number of photons collected by the detector. However, when the detected signal has amplitude which is close to the electronic noise floor, then the contribution of electronic noise to image quality degradation becomes an issue. Such scenarios can happen when doing scans at very low dose levels, which could be the case in exams such as low dose chest CT for lung cancer screening [30] or CT colonography [31] [32]; but also in scenarios when morbidly obese patients are scanned [33] [34], , i.e. causing photon starvation. **Fig. 2** provides an example of the noise reduction achieved with the use of the integrated electronics detector.

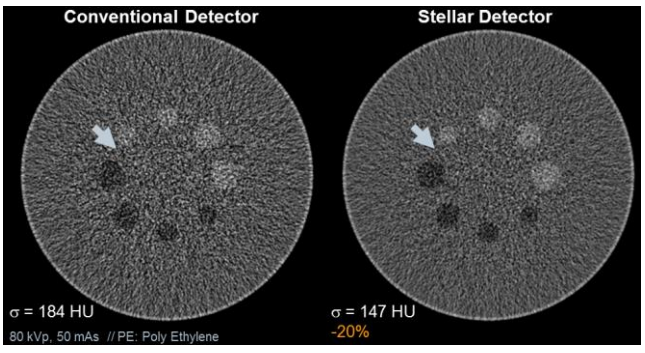

Fig. 2. Poly ethylene phantom scanned with identical CT technique of 80 kVp and 50 mAs using both a (left) conventional CT detector and (right) integrated-electronics detector (Stellar detector) to demonstrate noise reduction.

A commercial implementation of this new integrated detector electronics technology has been recently

introduced with the Stellar® and Stellar-Infinity ® detectors (Siemens Healthcare, Forchheim, Germany). Recently published investigations have confirmed the benefits of the integrated detectors for reducing the image noise when scanning obese patients or through the thicker anatomical cross-sections such as the shoulders and pelvis [34].

In addition to better dose efficiency by reducing electronic noise, advances in CT detectors can have a direct influence on spatial resolution by minimizing detector to detector crosstalk and coupling that information with more advanced iterative reconstruction methods which model system parameters such as focal spot blurring and detector themselves. For example, combining use of the Stellar detectors and iterative reconstruction lead to improvements in spatial resolution as demonstrated for applications such as temporal bone imaging [35] or for the depiction of coronary stents in CT angiograms [36], with both types of applications benefiting from the improved ability to depict smaller structures.

III. System Control of CT Parameters: Tube Current and Tube Potential

Automatic exposure control

The automatic exposure control (AEC) of the tube current in a CT scanner is one of the key features for radiation dose optimization, and it has become a standard feature in all modern CT systems. The AEC modulates the tube current as a response to changes in patient attenuation due to patient size, anatomy and shape [37] [38] [39]. The tube current can be modulated angularly, such that a higher current is applied in view angles with higher attenuation. For example, most patients are thicker (more attenuating) in the lateral direction relative to the anterior-posterior direction; hence a higher tube current is applied laterally relative to anterior-posterior. The tube current can also be modulated longitudinally. For example, patients typically have thicker cross-sections in the shoulders compared to the rest of the thorax that has less tissue because of the air-filled lungs. Hence, the longitudinal tube current modulation will apply a higher current through the shoulders and a lower current through the rest of the chest. One of the strategies used to perform AEC is CAREDose4D (Siemens Healthcare, Forchheim, Germany), which responds directly to attenuation changes from the patient in the angular direction (x-y plane) and also along the patient in the z-direction (**Fig. 3**). Furthermore, CAREDose4D has a built-in "real-time" feedback mechanism to further refine angular tube current modulation during the scan using the patient attenuation profile obtained from the previous 180 degrees of projection data.

Manufacturers use one of three main strategies to control the tube current in AEC systems: reference mAs (Siemens), standard deviation or noise index (Toshiba, General Electric, Hitachi), and reference image (Philips, Neusoft) [40]. For example, CAREDose4D is controlled with the reference effective mAs, with effective mAs defined as:

Eff. mAs = [tube current x rotation time] / pitch (1).

The reference effective mAs is defined as the effective mAs needed to produce the desirable image quality for a given reference attenuation (e.g. 33.9 cm of water for the abdomen (**Fig. 4**). If a patient has lower attenuation than the "reference patient", the effective mAs needed to reach the desired image quality is then lower than the reference effective mAs. On the contrary, larger patients will require an increase in the effective mAs beyond the reference value to warrant adequate image quality..

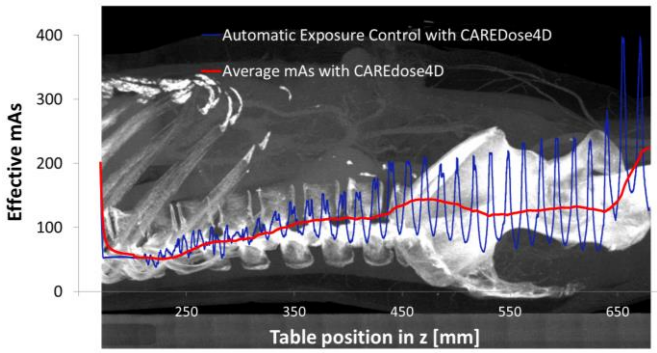

Fig. 3. Automatic exposure control of the tube current using CAREDose4D from a patient undergoing a chest-abdomen-pelvis CT exam. The tube current continuously changes as a function of patient's attenuation; hence it follows changes angularly and longitudinally, in addition to real-time feedback (every half rotation) to fine tune the tube current applied to the patient.

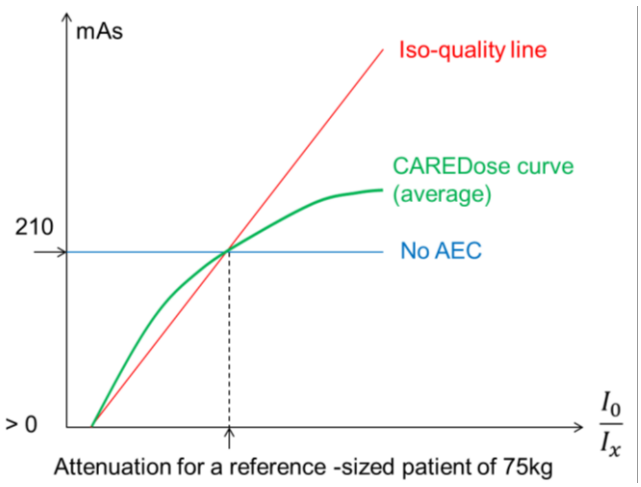

Fig. 4. Tube current-time product (mAs) adaptation as a function of patient attenuation. The example compares the nonlinear function used by CAREDose4D for automatic exposure control (AEC), with a fixed tube current approach (No AEC), and to a the tube current adaptation approach that attempts to deliver constant noise (iso-quality line).

Now, a mathematical function needs to be defined to adapt the effective mAs as a function of patient attenuation. One approach to that mathematical function is to linearly adapt the effective mAs with patient attenuation changes, such that the noise is constant. However, clinical experience

suggests that this relationship does not need to be linear, as higher noise can be tolerated in larger patients, due to more body fat that increases tissue contrast. Likewise, in pediatric applications the lack of intrinsic tissue contrast and the small structures may require lower image noise relative to adult patients. CAREDose4D operates under this paradigm, and hence, the relationship between patient's attenuation and applied tube current is nonlinear (**Fig. 4**). Furthermore, CAREDose4D allows the user to adjust the shape of the mathematical function to adapt the tube current to the patient attenuation. In practice, the users can define how aggressively they want to increase (or decrease) the tube current (i.e. effective mAs) in response to the changing patient attenuation.

Organ-based tube current modulation

Organ-based tube current modulation is designed to reduce the radiation exposure to superficial radiosensitive organs such as the breast [41] [42], thyroid [43] or the eye lens [44]. This technique is implemented as X-CARE (Siemens Healthcare, Forchheim, Germany) and operates by decreasing the tube-current when the x-ray tube is passing anteriorly to the patient in an angular range of about 120 degrees (**Fig. 5**). To avoid a compromise in image quality, the tube current is increased for the posterior angular range such that the overall radiation exposure is comparable to a traditional scan without X-CARE. Various investigators have found that organ-based tube current modulation can effectively spare radiation dose to sensitive organs like the breast [41] [45], eye lens [44], and thyroid [43]; while maintaining image quality in terms of image noise and CT number accuracy. An approach previously used to reduced exposure to radiosensitive and superficial organs were the bismuth shields, placed over the radiosensitive organ (e.g. on the breast), but they were found to have issues such as increased image noise and artifacts. The usage of bismuth shields has been controversial [46] [47] but it is now usually discouraged since a global reduction in the tube current or the use of technologies such as X-CARE can achieve the same goal without sacrificing image quality [48].

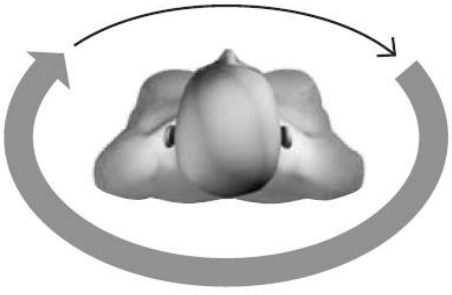

Fig. 5. Illustration of principle of organ-based tube current modulation with X-CARE. With this technology it is possible to reduce the exposure to radiosensitive organs such as the breast, thyroid or eye lens. This is achieved by decreasing the tube current by 75% of the maximum value while the x-ray tube is covering an anterior angular range of 120 degrees (thinner arrow) and then increased for the remaining view angles (thicker arrow).

Automated Tube Potential Selection

The selection of the tube potential in a CT examination has three main consequences. First, the tube potential influences the radiation exposure, with a relationship defined by $[kV_{new}/kV_{old}]^n$, where n is between 2 and 3 (depending on the patient's size). Second, because the tube potential affects the overall radiation exposure, the image noise is also affected; the lower the radiation exposure the higher the image noise. Therefore, the tube current typically has to be adjusted to compensate for an excessive increase in image noise when lowering the tube potential. The third consequence of changing the tube potential is that it directly impacts the image contrast of radiological relevant tissues and materials such as calcium and iodine. For either of those two materials, their contrast relative to soft tissue increases with reduced tube potential.

Various scientific studies have been done investigating the benefits of using lower tube potential, particularly for applications using iodinated contrast agents [49] [50]. One approach attempts to quantify the gain in image quality (i.e. CNR) while at the same time establish the dose efficiency by calculating a figure of merit, based on the square of the CNR and the radiation output, the dose weighted CNR (CNRD):

$$CNRD = \frac{(C_{iodine} - C_{water})^2}{\sigma^2 \cdot CTDI_{vol}}$$

Using the CNRD it is possible to demonstrate that for imaging tasks that use iodine, typically the use of tube potentials below 120 kVp can lead to improved dose efficiency, that is, a higher CNR at a lower dose (**Fig. 6**).

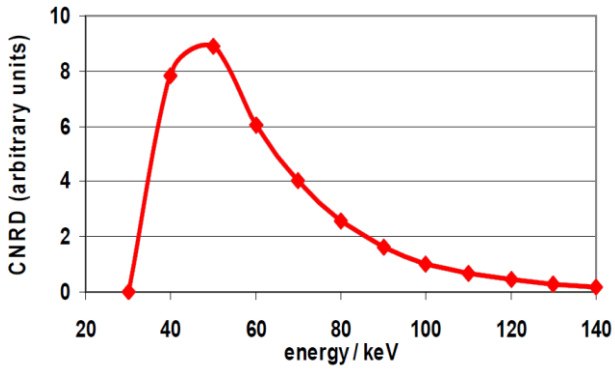

Fig. 6. Dose-weighted contrast to noise ratio (CNRD) as a function of photon energy (keV) for iodine relative to water. Since the mean energy of a polychromatic CT spectrum decreases with kVp, optimal CNRD is often found for lower kVp values (e.g 80 or 100 kVp) when the material's attenuation increases at lower energy values.

One challenge people often face when trying to effectively implement the consistent use of reduced tube potential is how to simultaneously adjust the tube current. Moreover, it is also necessary to consider the patient size, since practical issues such as the tube power limit may prevent the use of reduced tube potential for very large patients [49]. While many hospitals have experience with setting the quality reference mAs for conventional 120 kVp

examinations with AEC; this is often not the case when using a reduced tube potential such as 80 or 100 kVp. Therefore, users are more uncertain about which reference mAs should be used to maintain a desired level of image quality. One possible solution is to create comprehensive look-up tables or manual charts. However, this approach could be difficult to implement in a busy clinical environment and it could also be error prone. A more effective approach would be the ability to automatically select the tube potential [51]. One commercially available solution is CARE kV (Siemens Healthcare, Forchheim, Germany) that automatically selects the combination of tube potential and tube current according to patient size and diagnostic task.

The input to CARE kV consists of the patient CT localizer radiograph (i.e. topogram) and the user selection of an optimization setting based on the exam type (e.g. non-contrast, contrast-enhanced or angiography). Based on this input, CARE kV calculates the patient's attenuation and establishes a desired CNR associated with the diagnostic task selected. Then, CARE kV compares all combinations of tube potential and corresponding tube current values that reach the target CNR, and selects the combination that achieves this task at the lowest radiation output (i.e. $CTDI_{vol}$). For smaller patients, the system would typically select lower tube potential values, especially for contrast-enhanced examinations; while for larger patients the value often remains at 120 kVp. Furthermore, for non-contrast examinations in obese patients, CARE kV may suggest to increase the tube potential from 120 to 140 kVp, because the CNR might be slightly improved at 140 kVp due to less image noise at the same contrast.

Various studies using CARE kV have demonstrated substantial dose reductions ranging from 20 to 60% relative to scanning with 120 kVp. These dose reductions were achieved while maintaining or even improving image quality in CT applications such as CT angiography [52], contrast-enhanced body imaging applications [53], cardiac CT [54], and pediatric CT examinations [55].

IV. Iterative reconstruction

Iterative reconstruction (IR) has quickly become a standard feature on modern CT scanners, considering that first commercial implementations started to appear by 2009. The goal of using IR is to be able to acquire CT data with lower radiation exposure (e.g. by reducing mAs or kV) while maintaining image quality (e.g. image noise, spatial resolution, low-contrast detectability, etc.) and overall diagnostic performance similar to conventional filtered backprojection (FBP) reconstruction from higher dose CT data. Unlike FBP, IR can incorporate more information in the reconstruction process by modeling the system geometry, imposing smoothing constraints (i.e. regularization), and by incorporating physical effects such as beam hardening or scattering [56] [24] [57]. Implementing these aforementioned aspects of IR can result in very long reconstruction times and make IR of limited use in a busy clinical environment. The first generation IR methods have concentrated only on the regularization aspect (i.e. noise reduction). One of those techniques was Iterative Reconstruction in Image Space (IRIS, Siemens Healthcare, Forchheim, Germany) which incorporates a noise model to preserve spatial resolution and reduce image noise. The second generation IR methods began to improve noise modeling in the image space while also incorporating a feedback loop (i.e. forward projection) in the projection (raw) data domain to reduce artifacts caused by the non-exact (in mathematical sense) nature of FBP. This is the case of Sinogram Affirmed Iterative Reconstruction (SAFIRE, Siemens Healthcare, Forchheim, Germany), which achieves both noise reduction and artifact suppression [58]. SAFIRE has been combined with reduced tube current and reduced tube potential acquisition to increase the dose reduction potential [59] while maintaining image quality (**Fig. 7**).

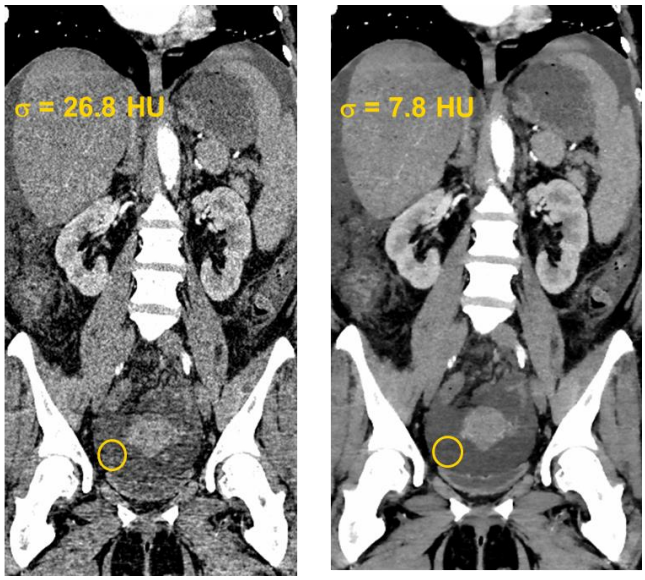

Fig. 7. Example comparing image reconstruction of the same CT dataset using (left) standard filtered back-projection (FBP) and (right) iterative reconstruction with SAFIRE. The dataset corresponds to a abdomen-pelvis examination of an adult patient. The image reconstructed with SAFIRE exhibits a lower noise, better CNR at maintained spatial resolution compared to the same image reconstructed with standard FBP.

Most recently, third generation IR methods have emerged, in which more detailed modeling in the projection data domain results in less noise streaks and better artifact suppression; while the improved three-dimensional regularization process results in better noise reduction in the image domain. An example of the third generation IR is the recently introduced Advance Modeled Iterative Reconstruction (ADMIRE, Siemens Healthcare, Forchheim, Germany). A combination of ADMIRE with other scanner advances has already demonstrated the potential for

dramatic dose reductions in applications such as lung cancer screening. For example, a recent phantom study using the SOMATOM Force and ADMIRE showed that image quality and CT number accuracy were maintained using a $CTDI_{vol}$ of only 0.15 mGy, which is comparable to the exposure of two-view chest radiographs [60].

A large number of publications have reported the effectiveness of IR methods to reduce image noise of lower dose acquisitions. This is prevalent across manufacturers who currently offer one or more types of IR approaches. However, due to the nonlinear nature of IR there is a greater awareness that simple metrics of noise reduction or CNR are insufficient to fully characterize these methods. Other effects such as noise power spectra, spatial resolution, and viewer conditions may affect the actual human observer performance. Several research groups have been putting serious efforts in the development of model observers to attempt to better characterize the actual radiation dose reduction potential of IR for various diagnostic tasks, most notably for low-contrast detectability [61] [62] [63] [64].

V. Application-specific technologies for dose optimization

Cardiac CT

There exist two major approaches for imaging the heart with CT: retrospective ECG-gating with a spiral CT acquisition and prospective ECG-triggering with a sequential CT acquisition (**Fig. 8**). One standard feature for dose reduction in the retrospective mode is to modulate the tube current to a lower value outside of a predefined cardiac phase of interest [65]. For example, in most cardiac examinations (heart rate ≤ 65 beats per minute) the optimal cardiac phase is around 70% (measured between two R peaks in the ECG signal), coinciding with mid to late diastole, which is when the heart is moving the least. Thus, with this technique the tube current is only maintained at its maximum value near the 70% phase: for example in a temporal window between 60 to 80%, while the tube current can be decreased to a lower value (i.e. 20% of the maximum tube current) outside this 60-80% cardiac phase range. The cardiac phase range corresponding to the maximum tube current window can be narrowed or widened according to the user needs and this will directly impact the total exposure delivered to the patient. One modern approach to this technique is the adaptive ECG-pulsing (Siemens Healthcare, Forchheim, Germany); in which the dose modulation for a cardiac scan is ECG-controlled. The ECG-pulsing algorithm is able to quickly react (by widening the acquisition window) when detecting an arrhythmia or ectopic beats so that image quality is maintained. This technique is recommended for patients with higher and unstable heart rates. On the other hand, a related innovation for this type of cardiac acquisition is to reduce the tube current outside the pre-defined acquisition window to only 4% of its maximum value (MinDose, Siemens Healthcare, Forchheim, Germany). With this type of ECG-based current modulation, it is possible to reduce mean radiation dose by up to 50% [65] relative to the acquisition without tube current modulation.

The prospectively triggered technique typically uses a sequential acquisition instead of spiral. Just like with the retrospective mode, the ECG signal is used to define a desired cardiac phase, but unlike to the retrospective mode, the x-rays are only applied during the cardiac phase of interest. Hence rather than decreasing the tube current to a lower value, the x-rays are turned off during the non-selected cardiac phase range. However, this mode traditionally works best for patients with relatively low and stable heart rates. An implementation of this type of cardiac CT acquisition is available as Adaptive Cardio-Sequence (Siemens Healthcare, Forchheim, Germany). This mode achieves more robust performance in cases with occasional ectopic beats by using an improved arrhythmia detection algorithm. With the use of these technologies, typical effective doses in the range of 1 to 3 mSv have been reported [66].

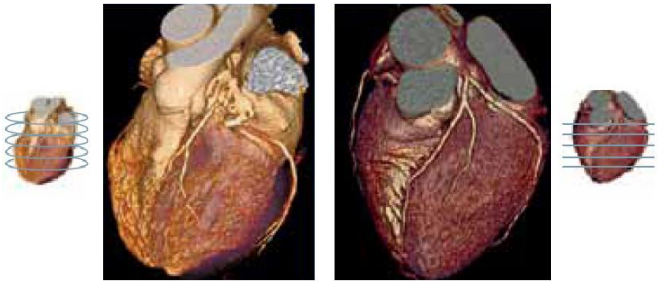

Fig. 8. Illustration of cardiac CT data acquired using adaptive ECG-pulsing in spiral CT (left) and with the adaptive cardio sequence (right) using a SOMATOM Definition dual-source CT system.

Ultra-fast scanning: Dual-source high-pitch technique for prospectively triggered cardiac CT

This technique is enabled by the use of the dual-source CT in which it is possible to operate the scanner with a high-pitch value of 3.4; which doubles the maximum pitch of 1.5-1.7, traditionally possible in conventional single-source CT system [67]. The basic principle of the high-pitch scan mode is that gaps in the projection data generated from one x-ray source are filled up by the data generated from the second x-ray source which is arranged perpendicularly to the first in a dual-source CT system (**Fig. 9**). Because no redundant data is acquired, this mode can reduce dose even further compared to the prospective sequential mode, while maintaining the image quality [68]. With this technique, it is possible to image the entire heart within one heart beat with excellent temporal resolution and often with less than 1 mSv effective dose when used in combination with lower tube potential such as 100 kVp [69]. The best image quality is achieved in patients with stable heart rates ≤ 60-65 bpm (SOMATOM Definition Flash) and ≤ 70-75 bpm (SOMATOM Force).

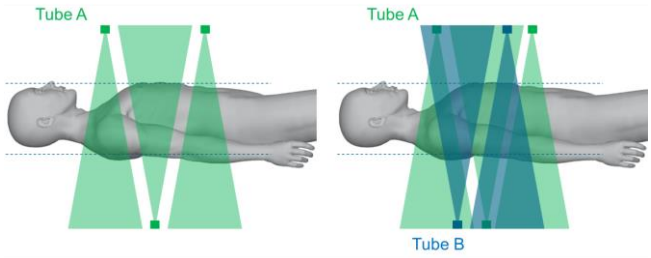

Fig. 9. Principle of high-pitch dual-source CT. A high-pitch value of up to 3.4 can be reached. The projection data gaps generated from projections recorded from exposure with one of the x-ray tubes (Tube A) are filled up with projections acquired from exposure from the second x-ray tube (tube B). Both x-ray tubes are arranged perpendicularly within the CT gantry. Dashed lines indicated the field of view in which image data is reconstructed (e.g. 33 cm in the SOMATOM Definition Flash dual-source CT).

Dual-Energy CT

In dual-energy CT two datasets are simultaneously acquired using two different tube potentials, most commonly 80/140 and 100/140 kVp. An advantage of using dual-energy CT over conventional single-energy CT is that in addition to anatomical imaging, it is possible to discriminate between some materials. Material decomposition with dual-energy CT is primarily based on expressing the attenuation coefficient of a voxel as a linear combination of the attenuation coefficients of two basis materials. This calculation can be done in either projection space or image space [70]. Because material decomposition allows the identification and quantification of materials such as iodine in the CT images, it is also possible to 'virtually' remove the iodine from the images and generate the so-called virtual-non contrast images. In multiple-phase CT studies, such as those commonly performed for imaging the liver or kidneys, virtual-non contrast imaging with dual-energy CT can potentially reduce the radiation exposure by 50 or 33%, in two- or three-phase CT studies. These radiation dose savings are achieved by eliminating the need of the true non-contrast CT images and replacing them with the virtual-non contrast images derived from post-contrast dual-energy CT exam [71] [72].

Another possibility for radiation dose reduction and image quality optimization is the use of virtual monoenergetic (or monochromatic) images calculated from dual-energy CT datasets [70]. Early studies demonstrated that virtual monoenergetic images can provide improved image quality at the same or lower dose when comparing to single-energy CT at 120 kVp [73]. A more recent study, using a new advanced version of monoenergetic imaging (Monoenergetic Plus, Siemens Healthcare), has demonstrated that it can actually provide superior CNR at the same dose compared to scanning with reduced tube potential at 80 kVp; and hence, can potentially reduce radiation dose [74].

VI. STANDARD ATTRIBUTES FOR DOSE OPTIMIZATION AND MANAGEMENT IN CT

In 2013, the national electrical manufacturers association (NEMA) released a set of standards which are expected to become commonplace in all CT scanners [75]. The released standard covers 4 aspects: (1) the use of standard DICOM structured reports to capture post-exam information regarding the radiation exposure such that it can be included in patient records; (2) dose check features that allow the users to set dose notifications and alerts (**Fig. 10**) that are used to inform the user that a predefined 'maximum' radiation output has been reached either for a given scan (dose notification) or the entire exam (dose alert). In case of the dose notification the scanner will inform the user that this maximum has been reached with a message box. In case of the dose alert a warning will also pop up but for the dose alert, the user will have to write down the reason why the dose is exceeded (i.e. clinically justified); (3) existance of reference pediatric and adult protocols stored into the scanner such that they are immediately available after installation; and (4) automatic exposure control needs to be available as one of the essential features for radiation dose optimization.

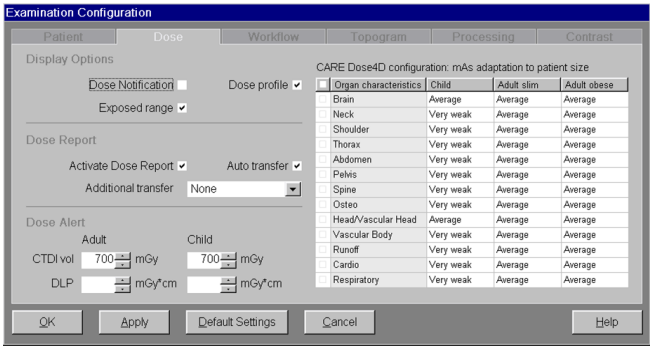

Fig. 10. Screenshot of the dose configuration screen in a Siemens CT system. This page is used to set up dose notifications and dose alerts, among others. When set up values are reached during an examination, the scanner will display the corresponding notifications or alerts to inform the user that a threshold has been reached. In the case of the dose alert, the user will need to write down an explanation why the value has been exceeded (i.e. medical reason) in order to continue the CT examination. In the US, the FDA suggested that the default value for dose alert be set at 1000 mGy.

VII. CONLUSIONS

We reviewed recent technological advances impacting each of the key components of the CT imaging chain starting from its essential hardware components, the systems control of key variables such as tube current and potential, and the image reconstruction engine. These advances help to tailor the CT examination to individual patients but also to different diagnostic tasks. Furthermore, we reviewed how specific technologies are modified to optimize image quality and reduce radiation dose in advanced applications such as cardiac CT, ultra-fast scanning, or dual-energy CT. It is

recommended that radiologists, medical physicists, and CT technologists become aware of these newer technologies and make use of them to benefit patients.

These new technologies provide more opportunities for automation in the selection of technique parameters. This becomes increasingly important for consistency in everyday practice, particularly in busy environments. In addition, newer tools such as dose structured reports, dose notifications and alerts (when properly set up) can aid in monitoring radiation exposures and avoiding errors.

REFERENCES

[1] G. N. Hounsfield, "Computerized transverse axial scanning (tomography). 1. Description of system," *British Journal of Radiology*, vol. 46, no. 552, pp. 1016-1022, 1973.

[2] W. A. Kalender, W. Seissler, E. Klotz and P. Vock, "Spiral volumetric CT with single-breath-hold technique, continuous transport, and continuous scanner rotation," *Radiology*, vol. 176, no. 1, pp. 181-183, 1990.

[3] K. Klingenbeck-Regn, S. Schaller, T. Flohr, B. Ohnesorge, A. Kopp and U. Baum, "Subsecond multi-slice computed tomography: basics and applications," *European Journal of Radiology*, vol. 31, pp. 110-124, 1999.

[4] C. H. McCollough and F. E. Zink, "Performance evaluation of a multi-slice CT system," *Medical Physics*, vol. 26, pp. 2223-2230, 1999.

[5] T. G. Flohr, C. H. McCollough, H. Bruder, M. Petersilka, K. Gruber, C. Suss, M. Grasruck, K. Stierstorfer, B. Krauss, R. Raupach, A. N. Primak, A. Kuttner, S. Achenbach, C. Becker, A. Kopp and B. M. Ohnesorge, "First performance evaluation of a dual-source CT (DSCT) system," *European Radiology*, vol. 16, pp. 256-268, 2006.

[6] F. Morsbach, S. Gordic, L. Desbiolles, D. Husarik, T. Frauenfelder, B. Schmidt, T. Allmendinger, S. Wildermuth, H. Alkadhi and S. Leschka, "Performance of turbo high-pitch dual-source CT for coronary CT angiography: first ex vivo and patient experience," *European Radiology*, 2014.

[7] M. Petersilka, H. Bruder, B. Krauss, K. Stierstorfer and T. Flohr, "Technical principles of dual source CT," *European Journal of Radiology*, vol. 68, pp. 362-368, 2008.

[8] NCRP, "Ionizing radiation exposure of the population of the United States. NCRP report No. 160.," National Council on Radiation Protection and Measurements, Bethesda MD, 2009.

[9] ACR, "Appropriateness Criteria. Guidelines.," American College of Radiology, 2014. [Online]. Available: http://www.acr.org/Quality-Safety/Appropriateness-Criteria. [Accessed 2 9 2014].

[10] NRC, "Health risks from exposure to low levels of ionizing radiation: BEIR VII - Phase 2," National Academies Press, Washington, DC, 2006.

[11] C. H. McCollough, L. Guimaraes and J. G. Fletcher, "In defense of body CT," *American Journal of Roentgenology AJR*, vol. 193, pp. 28-39, 2009.

[12] C. H. McCollough, F. E. Zink, J. Kofler, J. S. Matsumoto, K. B. Thomas and A. D. Hoffman, "Dose optimization in CT: creation, implementation and clinical acceptance of size-based technique charts.," *Radiology*, vol. 225, p. 591, 2002.

[13] F. G. Meinel, C. Canstein, J. Schoepf, M. Sedlmaier, B. Schmidt, B. S. Harris, T. G. Flohr and C. DeCecco, "Image quality and radiation dose of low tube voltage 3rd generation dual-source coronary CT angiography in obese patients: a phantom study," *European Radiology*, vol. 24, pp. 1643-1650, 2014.

[14] P. Schardt, J. Deuringer, J. Freudenberger, E. Hell, W. Knupfer, D. Mattern and M. Schild, "New x-ray tube performance in computed tomography by introducing the rotating envelope tube technology," *Medical Physics*, vol. 31, no. 9, pp. 2699-2706, 2004.

[15] M. J. Siegel, J. C. Ramirez-Giraldo, C. Hildebolt, D. Bradley and B. Schmidt, "Automated low-kilovoltage selection in pediatric computed tomography angiography: phantom study evaluating effects on radiation dose and image quality," *Investigative Radiology*, vol. 48, no. 8, pp. 584-589, 2013.

[16] R. Gnannt, A. Winklehner, R. Goetti, B. Schmidt, S. Kollias and H. Alkadhi, "Low kilovoltage CT of the neck with 70 kVp: comparison with a standard protocol," *AJNR American Journal of Neuroradiology*, vol. 33, no. 6, pp. 1014-1019, 2012.

[17] M. Meyer, H. Haubenreisser, J. Schoepf, R. Vliegenthart, C. Leidecker, T. Allmendinger, R. Lehmann, S. Sudarski, M. Borggrefe, S. O. Schoenberg and T. Henzler, "Closing in on the K Edge: Coronary CT Angiography at 100, 80, and 70 kV—Initial Comparison of a Second- versus a Third-Generation Dual-Source CT System," *Radiology*, vol. In Press, 2014.

[18] C. H. McCollough, A. N. Primak, O. Saba, H. Bruder, K. Stierstorfer, R. Raupach, C. Suess, B. Schmidt, B. M. Ohnesorge and T. G. Flohr, "Dose performance of a 64-channel dual-source CT scanner," *Radiology*, vol. 243, no. 3, pp. 775-784, 2007.

[19] Y. Lin, R.-G. J. C, D. J. Gauthier, K. Stierstorfer and E. Samei, "An angle-dependent estimation of CT x-ray spectrum from rotational transmission measurements," *Medical Physics*, vol. 41, no. 6, p. 062104, 2014.

[20] A. N. Primak, J. C. Ramirez-Giraldo, X. Liu, L. Yu and C. H. McCollough, "Improved dual-energy material discrimination for dual-source CT by means of additional spectral filtration," *Medical Physics*, vol. 36, no. 4, pp. 1359-1369., 2009.

[21] A. N. Primak, J. C. Ramirez-Giraldo, C. D. Eusemann, B. Schmidt, B. Kantor, J. G. Fletcher and C. H. McCollough, "Dual-source dual-energy CT with additional tin filtration: Dose and image quality evaluation in phantoms and in vivo," *American Journal of Roentgenology AJR*, vol. 195, no. 5, pp. 1164-1174, 2010.

[22] S. Gordic, F. Morsbach, B. Schmidt, T. Allmendinger, T. Flohr, D. Husarik, S. Baumueller, R. Raupach, P. Stolzmann, S. Leschka, T. Frauenfelder and H. Alkadhi, "Ultralow-dose chest computed tomography for pulmonary nodule detection: first performance evaluation of single energy scanning with spectral shaping," *Investigative Radiology*, vol. 49, no. 7, pp. 465-473, 2014.

[23] J. Hsieh, Computed Tomography: Principles, design, artifacts, and recent advances, Bellingham, MA: SPIE Press, 2006.

[24] L. Yu, X. Liu, S. Leng, J. M. Kofler, J. C. Ramirez-Giraldo, M. Qu, J. Christner, J. G. Fletcher and C. H. McCollough, "Radiation dose reduction in computed tomography: techniques and future perspective," *Imaging in Medicine*, vol. 1, no. 1, pp. 65-84., 2009.

[25] K. Stierstorfer, U. Kuhn, H. Wolf, M. Petersilka, C. Suess and T. G. Flohr, "Principle and performance of a dynamic collimation technique for spiral CT," in *Radiological Society of North America (RSNA)*, Chicago IL, 2007.

[26] J. A. Christner, V. A. Zavaletta, C. D. Eusemann, A. I. Walz-Flannigan and C. H. McCollough, "Dose reduction in helical CT: Dynamically adjustable z-axis x-ray beam collimation," *American Journal of Roentgenology AJR*, vol. 194, pp. W49-W55, 2010.

[27] P. Deak, O. Langner, M. Lell and W. A. Kalender, "Effects of adaptive section collimation on patient radiation dose in multisection spiral CT," *Radiology*, vol. 252, pp. 140-147, 2009.

[28] J. Paul, R. Banckwitz, B. Krauss, T. Vogl, W. Maentele and R. Bauer, "Estimation and comparison of effective dose (E) in standard chest CT by organ dose measurements and dose-length-product methods and assessment of the influence of CT tube potential (energy dependency) on effective dose in a dual-source CT," *European Journal of Radiology*, vol. 81, no. 4, pp. e507-e512, 2012.

[29] T. Fuchs, M. Kachelriess and W. Kalender, "Direct comparison of a xenon and a solid-state CT detector system: measurements under working conditions," *IEEE Transactions on Medical Imaging*, vol. 19, no. 9, p. 941, 2000 .

[30] D. D. Cody, H. J. Kim, C. H. Cagnon, F. J. Larke, M. M. McNitt-Gray, R. L. Kruger, M. J. Flynn, J. A. Seibert, P. F. Judy and X. Wu, "Normalized CT dose index of the CT scanners used in the National Lung Screening Trial," *American Journal of Roentgenology*, vol. 194, no. 6, pp. 1539-1546, 2010.

[31] Y. Liu, S. Leng, G. Michalak, T. Vrieze, X. Duan, M. Qu, M. Shiung, C. McCollough and J. Fletcher, "Reducing image noise in computed tomography (CT) colonography: effect of an integrated circuit CT detector," *Journal of Computer Assisted Tomography*, vol. 38, no. 3, pp. 398-403, 2014.

[32] J. G. Fletcher, K. L. Grant, J. L. Fidler, M. Shiung, L. Yu, J. Wang, B. Schmidt, T. Allmendinger and C. H. McCollough, "Validation of dual-source single-tube reconstruction as a method to obtain half-dose images to evaluate radiation dose and noise reduction: phantom and human assessment using CT colonography and sinogram-affirmed iterative reconstruction (SAFIRE)," *Journal of Computer Assisted Tomography*, vol. 36, no. 5, pp. 560-569, 2012.

[33] F. Morsbach, S. Bickelhaupt, S. Rätzer, B. Schmidt and H. Alkadhi, "Integrated circuit detector technology in abdominal CT: added value in obese patients," *American Journal of Roentgenology*, vol. 202, no. 2, pp. 368-374. , 2014.

[34] X. Duan, J. Wang, S. Leng, B. Schmidt, T. Allmendinger, K. Grant, T. Flohr and C. McCollough, "Electronic noise in CT detectors: Impact on image noise and artifacts," *American Journal of Roentgenology AJR*, vol. 201, no. 4, pp. W626-W632, 2013.

[35] C. H. McCollough, S. Leng, J. Sunnegardh, T. J. Vrieze, L. Yu, J. Lane, R. Raupach, K. Stierstorfer and T. G. Flohr, "Spatial resolution improvement and dose reduction potential for inner ear CT imaging using a z-axis deconvolution technique," *Medical Physics*, vol. 40, no. 6, p. 61904, 2013.

[36] F. Morsbach, L. Desbiolles, A. Plass, S. Leschka, B. Schmidt, V. Falk, H. Alkadhi and P. Stolzmann, "Stenosis quantification in coronary CT angiography: impact of an integrated circuit detector with iterative reconstruction.," *Investigative Radiology*, vol. 48, no. 1, pp. 32-40, 2013.

[37] M. K. Kalra, M. M. Mahe, T. L. Toth, B. Schmidt, B. L. Westerman, H. T. Morgan and S. Saini, "Techniques and applications of automatic tube current modulation for CT," *Radiology*, vol. 233, no. 3, pp. 649-657, 2004.

[38] M. Gies, W. A. Kalender, H. Wolf and C. Suess, "Dose reduction in CT by anatomically adapted tube current modulation. I. Simulation studies.," *Medical Physics*, vol. 26, pp. 2235-2247, 1999.

[39] W. A. Kalender, H. Wolf and C. Suess, "Dose reduction in CT by anatomically adapted tube current modulation. II. Phantom measurements," *Medical Physics*, vol. 26, pp. 2248-2253, 1999.

[40] AAPM, "CT scan parameters: Translation of terms for different manufacturers," American Association of Physicists in Medicine AAPM, 20 April 2012. [Online]. Available: https://www.aapm.org/pubs/CTProtocols/. [Accessed 02 September 2014].

[41] S. V. Vollmar and W. A. Kalender, "Reduction of dose to female breast in thoracic CT: a comparison of stardard-protocol, bismuth-shielded, partial and tube-current-modulated CT examinations," *European Radiology*, vol. 18, pp. 1674-1682, 2008.

[42] J. Wang, X. Duan, J. A. Christner, S. Leng, L. Yu and C. H. McCollough, "Radiation dose reduction to the breast in thoracic CT: comparison of bismuth shielding, organ-based tube current modulation, and use of a globally decreased tube current.," *Medical Physics*, vol. 38, no. 11, pp. 6084-6092, 2011.

[43] J. K. Hoang, T. T. Yoshizumi, K. R. Choudhury, G. B. Nguyen, G. Toncheva, A. R. Gafton, J. D. Eastwood, C. Lowry and L. M. Hurwitz, "Organ-based dose current modulation and thyroid shields: techniques of radiation dose reduction for neck CT.," *American Journal of Roentgenology AJR*, vol. 198, no. 5, pp. 1132-1138, 2012.

[44] J. Wang, X. Duan, J. A. Christner, S. Leng, K. L. Grant and C. H. McCollough, "Bismuth shielding, organ-based tube current modulation, and global reduction of tube current for dose reduction to the eye at head CT," *Radiology*, vol. 262, no. 1, pp. 191-198, 2012.

[45] M. P. Lungren, T. T. Yoshizumi, S. M. Brady, G. Toncheva, C. Anderson-Evans, C. Lowry, X. R. Zhou, D. Frush and L. M. Hurwitz, "Radiation dose estimations to the thorax using organ-based dose modulation.," *American Journal of Roentgenology AJR*, vol. 199, no. 1, pp. W65-W73, 2012.

[46] C. H. McCollough, J. Wang, R. G. Gould and C. G. Orton, "Point/counterpoint.The use of bismuth breast shields for CT should be discouraged.," *Medical Physics*, vol. 39, no. 5, pp. 2321-2324, 2012.

[47] P. M. Colletti, O. A. Micheli and K. H. Lee, "To Shield or Not to Shield: Application of Bismuth Breast Shields," *American Journal of Roentgenology AJR*, vol. 200, no. 3, pp. 503-507, 2013.

[48] AAPM, "Board of Directors. AAPM position statement on the use of bismuth shielding for the purpose of dose reduction in CT scanning. Policy PP-26-A.," AAPM, 7 February 2012. [Online]. Available: www.aapm.org/publicgeneral/BismuthShielding.pdf. [Accessed 02 September 2014].

[49] W. A. Kalender, P. Deak, M. Kellermeier, M. Van Straten and S. V. Vollmar, "Application- and patient size-dependent optimization of x-ray spectra for CT," *Medical Physics*, vol. 36, no. 3, pp. 993-1007, 2009.

[50] D. Marin, R. C. Nelson, H. Barnhart, S. T. Schindera, H. L. M, T. A. Jaffe, T. T. Yoshizumi, R. Youngblood and E. Samei, "Detection of pancreatic tumors, image quality, and radiation dose during the pancreatic parenchymal phase: effect of a low-tube-voltage, high-tube-current CT technique--preliminary results," *Radiology*, vol. 256, no. 2, pp. 450-459, 2010.

[51] L. Yu, H. Li, J. G. Fletcher and C. H. McCollough, "Automatic selection of tube potential for radiation dose reduction in CT: a general strategy," *Medical Physics*, vol. 37, no. 1, pp. 234-243, 2010.

[52] R. Goetti, A. Winklehner, S. Gordic, S. Baumueller, C. A. Karlo, T. Frauenfelder and H. Alkadhi, "Automated attenuation-based kilovoltage selection: preliminary observations in patients after endovascular aneurysm repair of the abdominal aorta," *American Journal of Roentgenology AJR*, vol. 199, no. 3, pp. W380-W385, 2012.

[53] C. Mayer, M. Meyer, C. Fink, B. Schmidt, M. Sedlmair, S. O. Schoenberg and T. Henzler, "Potential for radiation dose savings in abdominal and chest CT using automatic tube voltage selection in combination with automatic tube current modulation," *American Journal of Roentgenology AJR*, vol. 203, no. 2, pp. 292-299, 2014.

[54] C. Layritz, G. Muschiol, T. Flohr, C. Bietau, M. Marwan, A. Schuhbaeck, J. Schmid, D. Ropers, S. Achenbach and T. Pflederer, "Potential for radiation dose savings in abdominal and chest CT using automatic tube voltage selection in combination with automatic tube current modulation," *Journal of Cardiovascular Computed Tomography*, vol. 7, no. 5, pp. 303-310, 2013.

[55] M. J. Siegel, C. Hildebolt and D. Bradley, "Effects of automated kilovoltage selection technology on contrast-enhanced pediatric CT and CT angiography," *Radiology*, vol. 268, no. 2, pp. 538-547, 2013.

[56] J. B. Thibault, K. D. Sauer, C. A. Bouman and J. Hsieh, "A three-dimensional statistical approach to improved image quality for multislice CT," *Medical Physics*, vol. 34, pp. 4526-4544, 2007.

[57] D. Mehta, R. Thompson, T. Morton, A. Dhanantwari and E. Shefer, "Iterative model reconstruction: simultaneously lowered computed tomography radiation dose and improved image quality," *Medical Physics International Journal*, vol. 1, no. 2, pp. 147-155, 2013.

[58] H. Bruder, R. Raupach, J. Sunnegardh, M. Sedlmair, K. Stierstorfer and T. Flohr, "Adaptive Iterative," in *Proceedings of SPIE Medical Imaging*, San Diego, CA, 2011.

[59] G. S. Desai, J. M. Fuentes-Orrego, A. R. Kambadakone and D. V. Sahani, "Performance of iterative reconstruction and automated tube voltage selection on the image quality and radiation dose in abdominal CT scans," *Journal of Computer Assisted Tomography* , vol. 37, no. 6, pp. 897-903, 2013.

[60] J. D. Newell, M. K. Fuld, T. Allmendinger, J. P. Sieren, K. Chan, J. Guo and E. A. Hoffman, "Very Low-Dose (0.15 mGy) Chest CT Protocols Using the COPDGene 2 Test Object and a Third-Generation Dual-Source CT Scanner With Corresponding Third-Generation Iterative Reconstruction Software," *Investigative Radiology*, vol. In Press, 2014.

[61] E. Samei, S. Richard and L. Lurwitz, "Model-based CT performance assessment and optimization for iodinated and noniodinated imaging tasks as a function of kVp and body size," *Medical Physics*, vol. 41, no. 8, p. 081910, 2014.

[62] J. Solomon and E. Samei, "Quantum noise properties of CT images with anatomical textured backgrounds across reconstruction algorithms: FBP and SAFIRE," *Medical Physics*, vol. 41, no. 9, p. 091908, 2014.

[63] Y. Zhang, S. Leng, L. Yu, R. E. Carter and C. H. McCollough, "Correlation between human and model observer performance for discrimination task in CT," *Physics in Medicine and Biology*, vol. 59, no. 13, pp. 3389-3404, 2014.

[64] K. Li, J. Tang and C. G. H, "Statistical model based iterative reconstruction (MBIR) in clinical CT systems: experimental assessment of noise performance," *Medical Physics*, vol. 41, no. 4, p. 041906, 2014.

[65] T. F. Jakobs, C. R. Becker, B. Ohnesorge, T. Flohr, C. Suess, U. J. Schoepf and M. F. Reiser, "Multislice helical CT of the heart with retrospective ECG gating: reduction of radiation exposure by ECG-controlled tube current modulation," *European Radiology* , vol. 12, no. 5, pp. 1081-1086, 2002.

[66] P. Stolzmann, S. Leschka, H. Scheffel, T. Krauss, L. Desbiolles, A. Plass, M. Genoni, T. G. Flohr, S. Wildermuth, B. Marincek and H. Alkadhi, "Dual-source CT in step-and-shoot mode: noninvasive coronary angiography with low radiation dose," *Radiology*, vol. 249, no. 1, pp. 71-80, 2008.

[67] M. Petersilka, H. Bruder, B. Krauss, K. Stierstorfer and T. G. Flohr, "Technical principles of dual source CT," *European Journal of Radiology*, vol. 68, no. 3, pp. 362-368, 2008.

[68] T. G. Flohr, S. Leng, L. Yu, T. Allmendinger, H. Bruder, M. Petersilka, C. D. Eusemann, K. Stierstorfer, B. Schmidt and C. H. McCollough, "Dual-source spiral CT with pitch up to 3.2 and 75 ms temporal resolution: image reconstruction and assessment of image quality," *Medical Physics*, vol. 36, no. 12, pp. 5641-5653, 2009.

[69] M. Lell, M. Marwan, T. Schepis, T. Pflederer, K. Anders, T. Flohr, T. Allmendinger, W. Kalender, D. Ertel, C. Thierfelder, A. Kuettner, D. Ropers, W. G. Daniel and S. Achenbach, "Prospectively ECG-triggered high-pitch spiral acquisition for coronary CT angiography using dual source CT: technique and initial experience.," *European Radiology*, vol. 19, no. 11, pp. 2576-2583, 2009.

[70] L. Yu, J. A. Christner, S. Leng, J. Wang, J. G. Fletcher and C. H. McCollough, "Virtual monochromatic imaging in dual-source dual-energy CT: radiation dose and image quality," *Medical Physics*, vol. 38, no. 12, pp. 6371-6379, 2011.

[71] A. Graser, T. R. Johnson, E. M. Hecht, C. R. Becker, C. Leidecker, M. Staehler, C. G. Stief, H. Hildebrandt, M. C. Godoy, M. E. Finn, F. Stepansky, M. F. Reiser and M. Macari, "Dual-energy CT in patients suspected of having renal masses: can virtual nonenhanced images replace true nonenhanced images?," *Radiology*, vol. 252, no. 2, pp. 433-440, 2009.

[72] A. J. Megibow and D. Sahani, "Best practice: implementation and use of abdominal dual-energy CT in routine patient care," *American Journal of Roentgenology AJR*, vol. 199, no. 5, pp. S71-S77, 2012.

[73] S. Sudarski, P. W. Apfaltrer, J. Nance, D. Schneider, M. Meyer, S. O. Schoenberg, C. Fink and T. Henzler, "Optimization of keV-settings in abdominal and lower extremity dual-source dual-energy CT angiography determined with virtual monoenergetic imaging," *European Journal Radiology*, vol. 82, no. 10, pp. e574-e581, 2013.

[74] K. L. Grant, T. G. Flohr, B. Krauss, M. Sedlmair, C. Thomas and B. Schmidt, "Assessment of an advanced image-based technique to calculate virtual monoenergetic computed tomographic images from a dual-energy examination to improve contrast-to-noise ratio in examinations using iodinated contrast media.," *Investigative Radiology*, vol. 49, no. 9, pp. 586-592, 2014.

[75] NEMA, "NEMA XR 29-2013: Standard Attributes on CT Equipment Related," National Electrical Manufacturers Association, Rosslyn, VA, 2013.

Contacts of the corresponding author:

Author:	Juan C. Ramirez-Giraldo, PhD
Institute:	Siemens Medical Solutions USA, Inc
City:	Malvern PA
Country:	USA
Email:	juancarlos.ramirezgiraldo@siemens.com